

ARTICLE OPEN



MULTIPLE MYELOMA, GAMMOPATHIES

Senescence profiling of monoclonal gammopathies reveals paracrine senescence as a crucial defense against disease progression

Gabriel Alvares Borges^{1,15}, Marta Diaz-delCastillo^{2,3,15}, Angelo J. Guilatco^{1,4}, Bilal Mohamad El-Masri⁵, Fatima A. Mustapha², Michael T. Gundesen⁶, Maja Hinge⁷, Thomas Lund⁶, Nadine Abdallah¹, Linda B. Baughn⁸, Ming Xu⁹, Anne Gingery^{10,11}, Tamar Tchkonja¹², James L. Kirkland¹², Taxiarchis Kourelis¹, Matthew T. Drake¹³, Thomas Levin Andersen^{2,3,5,14,16} and Megan M. Weivoda^{1,11,16}✉

© The Author(s) 2025

Multiple myeloma (MM) is a plasma cell (PC) malignancy that is preceded by monoclonal gammopathy of undetermined significance (MGUS) and/or smoldering multiple myeloma (SMM). MGUS and SMM PCs exhibit the same primary oncogenic abnormalities as MM but lack the end-organ damage that defines proliferative disease, suggesting that clonal PCs in these precursor conditions could exhibit senescence or senescence-like growth arrest. Herein we identified monoclonal gammopathy patient-derived PCs that exhibit senescence features and found that senescent PCs were significantly increased in MGUS patients compared to SMM or MM. Spatial analysis of senescent PCs in stable MGUS and SMM patient biopsies demonstrated the activation of local paracrine senescence in the bone marrow microenvironment. Stable MGUS and SMM patients also exhibited disease-specific senescence-associated secretory phenotype (SASP) signatures that significantly correlated with PC burden and clonal antibody. In contrast, progressing MGUS, SMM, and new MM patients lacked local paracrine senescence responses and robust activation of disease specific SASP signatures. Overall, these data suggest that failure to activate tumor-specific paracrine senescence responses is key to disease progression in monoclonal gammopathies.

Leukemia (2025) 39:1206–1217; <https://doi.org/10.1038/s41375-025-02572-z>

INTRODUCTION

Multiple myeloma (MM) is a clonal plasma cell (PC) malignancy and the second most common hematologic cancer in the United States [1]. MM is preceded by the PC dyscrasias monoclonal gammopathy of undetermined significance (MGUS) and smoldering multiple myeloma (SMM) [2, 3]. Like MM, patients with MGUS and SMM exhibit elevated serum M-protein, an abnormal clonal PC-derived immunoglobulin; however, they lack the end-organ damage associated with PC proliferative diseases. The annual risk for progression of MGUS or SMM to MM is ~1% and 10%, respectively [4]. Most SMM patients progress to MM ≤ 5 y of diagnosis, after which the risk drops to 3%/y [5]. While there are risk stratification algorithms to classify patients at higher risk [6, 7], the ability to predict MGUS and SMM patients who will progress

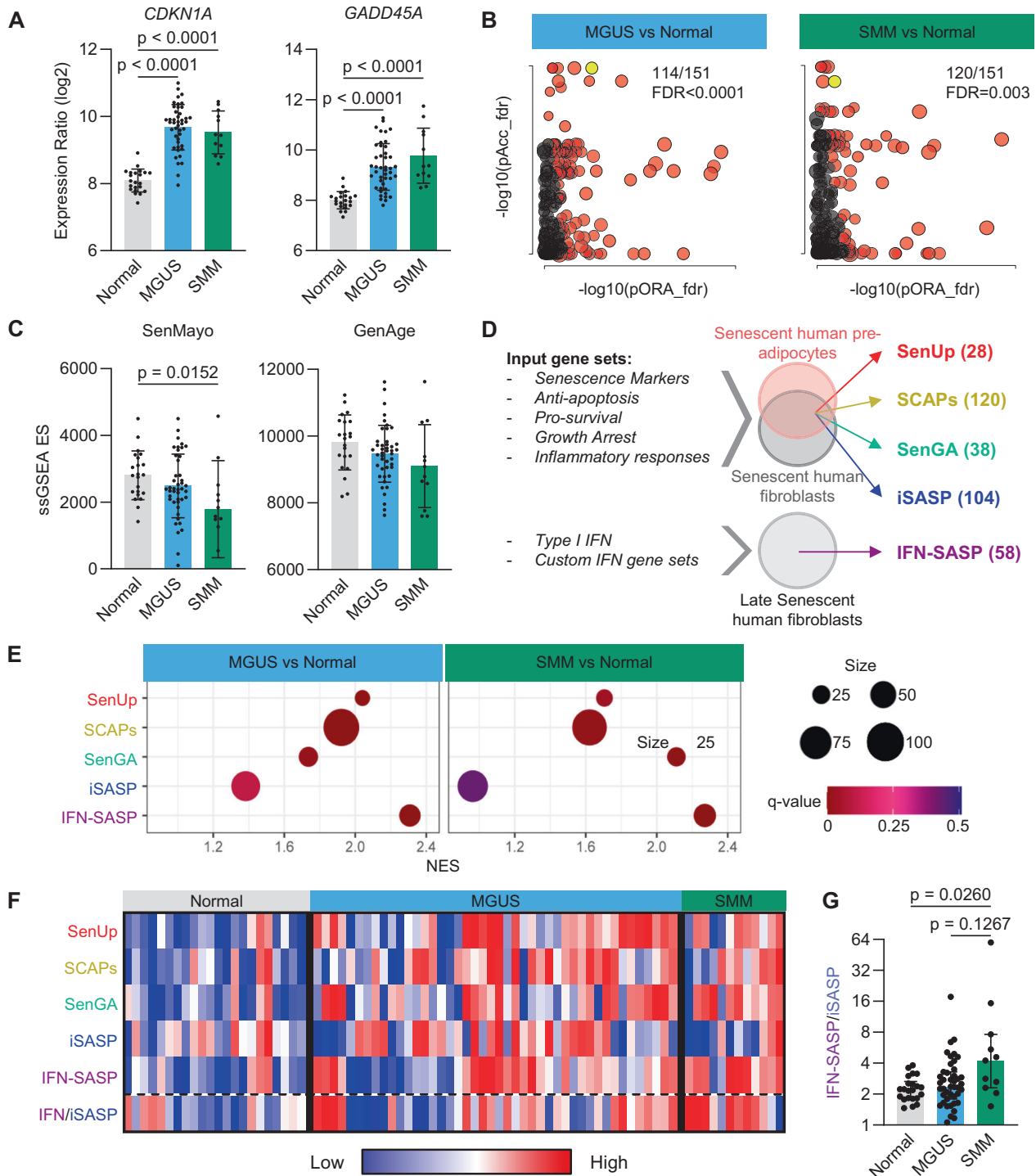
remains limited, hindering early intervention. The mechanisms by which MGUS and SMM progress to malignancy remain unclear, and there are currently no treatments to prevent disease progression.

While MGUS and SMM patients are generally asymptomatic, their pre-malignant PCs exhibit many of the same primary oncogenic abnormalities as MM cells [8–10]. The presence of primary oncogenic events with no/low proliferative capacity in MGUS and some SMM PCs, as opposed to MM PC proliferative disease, suggests that these cells could be in a senescent-like state of growth arrest. Cellular senescence is induced by cell stressors, such as oncogenic stress and DNA damage, and is crucial for preventing tumorigenesis. Senescent cells also exhibit a senescence-associated secretory phenotype (SASP) that reinforces

¹Mayo Clinic Division of Hematology, Rochester, MN, USA. ²University of Aarhus, Department of Forensic Medicine, Aarhus, Denmark. ³Danish Spatial Imaging Consortium (DanSIC), University of Aarhus and University of Southern Denmark, Aarhus, Denmark. ⁴University of Michigan, Cancer Biology Graduate Program, Ann Arbor, MI, USA. ⁵University of Southern Denmark, Odense, Denmark. ⁶Odense University Hospital, Department of Hematology, Odense, Denmark. ⁷Lillebaelt Hospital, Department of Hematology, Vejle, Denmark. ⁸Mayo Clinic Department of Laboratory Medicine and Pathology, Rochester, MN, USA. ⁹University of Minnesota Department of Biochemistry, Molecular Biology and Biophysics, Minneapolis, MN, USA. ¹⁰Mayo Clinic Department of Orthopedic Surgery, Rochester, MN, USA. ¹¹Mayo Clinic Department of Biochemistry and Molecular Biology, Rochester, MN, USA. ¹²Center for Advanced Gerotherapeutics, Cedars-Sinai Medical Center, Los Angeles, CA, USA. ¹³Hospital for Special Surgery Division of Endocrinology, New York, NY, USA. ¹⁴Odense University Hospital, Department of Clinical Pathology, Odense, Denmark. ¹⁵These authors contributed equally: Gabriel Alvares Borges, Marta Diaz-delCastillo. ¹⁶These authors jointly supervised this work: Thomas Levin Andersen, Megan M Weivoda. ✉email: thomas.levin.andersen@rsyd.dk; Weivoda.megan@mayo.edu

Received: 3 October 2024 Revised: 18 February 2025 Accepted: 14 March 2025

Published online: 31 March 2025



the senescence growth arrest in the surrounding microenvironment and drives immune activation to clear damaged and senescent cells [11, 12]. Together, senescence-induced growth arrest and SASP-induced immune clearance protect against the malignant transformation of damaged cells.

Consistent with this, senescence markers are present in pre-malignant lesions and can be detected prior to tumor formation in mice [13]. In contrast to the protective effects of senescence against tumorigenesis, senescent cell accumulation drives aging pathologies [14, 15], including promoting tumor progression [16]. The incidence of MGUS [17] and MM [18] increases with aging,

and obesity is a primary risk factor for the progression of MGUS and SMM to MM [19]. Of interest, both aging [20] and obesity [21] are associated with senescent cell accumulation. Moreover, retrospective studies have indicated that metformin, an anti-diabetic drug that inhibits the SASP [22], may prevent MGUS progression in diabetic patients [23, 24]. These apparently contradictory roles for senescence raise important questions regarding its role in pre-malignant monoclonal gammopathies and disease progression.

In this study, we used patient samples to demonstrate that MGUS and SMM PCs exhibit disease stage-specific senescence

Fig. 1 Enrichment of senescence-related gene sets in MGUS and SMM PCs after analysis of an independent previously published human gene array dataset (GSE5900). **A** Differential expression analysis of MGUS and SMM PCs revealed a significant upregulation of the senescence markers *CDKN1A* and *GADD45A*. Bars represent means with standard deviations (SD). *p* values were calculated using the one-way ANOVA test followed by Tukey's multiple comparisons test. **B** Advaita iPathway Guide analysis showed that the 'Cellular Senescence' pathway (yellow dot) was significantly enriched in both MGUS and SMM PCs. Dots represent individual pathways, plotted based on their *p*-value for perturbation accumulation (pAcc) versus overrepresentation analysis (pORA). Other significant combined *p*-values are shown in red. **C** Single sample GSEA (ssGSEA) using "GenAge" and "SenMayo" gene sets resulted in no enrichment in MGUS or SMM PCs, suggesting that senescence gene enrichment is independent of age-related senescence. **D** To customize senescence phenotyping gene sets, input gene sets were compiled and tested against two independent senescence gene expression datasets (GSE66236 and GSE109700). Genes that were significantly upregulated in both datasets were added to the relevant senescence gene sets. The IFN-SASP gene set was compiled with genes from existing IFN gene sets and tested against a late senescence RNA-seq dataset (GSE109700). "SenUp" = Senescence Up; SCAPs = Senescent Cell Anti-Apoptosis Pathways; SenGA = Senescence Growth Arrest; iSASP = Inflammatory Senescence-Associated Secretory Phenotype (SASP); IFN-SASP = Interferon-SASP. **E** GSEA analysis revealed significant enrichment (Normalized Enrichment Score - NES > 1.5, *q* < 0.05) of gene sets "SenUp", "SCAPs", "SenGA", and "IFN-SASP" in MGUS and SMM PCs, while the "iSASP" gene set was exclusively enriched in MGUS PCs (NES = 1.4, *q* = 0.11). **F** ssGSEA confirmed significant enrichment of senescence phenotyping gene sets throughout MGUS samples, with SMM samples showing enrichment in all gene sets except for "iSASP". **G** Calculation of "IFN-SASP"/"iSASP" enrichment ratios showed a significant increase in SMM samples compared to healthy donors, indicating a higher prevalence of IFN-related SASP in SMM. Bars represent medians with interquartile ranges. *p* values were calculated using the Kruskal-Wallis test followed by Dunn's multiple comparisons test.

features, as well as paracrine senescence responses that are most prominent in patients with stable disease. These findings support that robust activation of a paracrine senescence anti-tumor response is key to preventing malignant progression of monoclonal gammopathies.

RESULTS

MGUS and SMM PCs are enriched for senescence gene sets independently from aging

To test whether pre-malignant MGUS and SMM PCs exhibit gene expression consistent with senescence, we first performed a secondary analysis of a published human gene array dataset comparing healthy (*N* = 22), MGUS (*N* = 44), and SMM (*N* = 12) patient PCs; patient characteristics are summarized in Supplementary Table 1 [25].

Differential expression analysis revealed significant increases in senescence-related genes, including *CDKN1A* and *GADD45A* (Fig. 1A), in MGUS and SMM PCs compared to normal PCs. *CDKN1A* and *GADD45A* were previously identified as upregulated in a subset of stable MGUS (≥ 2.5 y, *N* = 19) patient PCs analyzed in the original study by Zhan et al. [25]. Pathway analysis (iPathwayGuide, Advaita) of differentially expressed genes revealed "Cellular Senescence" as the most significantly impacted pathway in MGUS PCs and significantly affected in SMM PCs compared to normal (Fig. 1B, Supplementary Table 2).

While age and sex were included in the published patient characteristics, information on healthy donors was limited. Since senescence genes, including *CDKN1A* and *GADD45A*, are also increased with biological aging, we sought to determine whether senescence pathway enrichment in MGUS and SMM PCs could be due to age differences compared to the normal donors. To this end we performed single sample GSEA (ssGSEA) using the "GenAge" gene set, a curated list of genes that change with biological aging (<https://genomics.senescence.info/genes/human.html>), as well as the "SenMayo" gene set, which was documented to correlate with the age-related accumulation of senescent cells [26]. Using a publically available human bone marrow single cell RNA-sequencing dataset (GSE120446) [27], we confirmed the PC subsets from donors >65 y have significant enrichment of "SenMayo" and "GenAge" compared to donors <40 y (Supplementary Fig. 1). Neither MGUS nor SMM PCs exhibited enrichment for "GenAge" or "SenMayo" (Fig. 1C); in fact, SMM PCs exhibited significantly decreased enrichment for "SenMayo" compared to healthy donors. Thus, senescence pathway enrichment in MGUS and SMM PCs appears to be distinct from age-related senescence based on the lack of enrichment of biological aging gene sets.

We next sought to create senescence phenotyping gene sets for GSEA to characterize senescence in MGUS and SMM PCs. For this, we compiled existing senescence gene sets and gene lists related to senescence phenotypes. Custom lists were tested against two published datasets of human pre-adipocytes [28] or fibroblasts [29] in which senescence was induced and validated in vitro, allowing for the identification of central senescence genes that are shared across cell lineages. Genes from input lists that were significantly induced in both senescence datasets were added to our senescence phenotyping gene sets based on the source list. To account for variable SASP phenotypes, particularly the late-senescence-associated interferon (IFN)-SASP, we compiled genes from existing IFN gene sets and tested these against a late-senescence RNA-seq dataset [29]. Using this strategy, we created the following senescence phenotyping gene sets: "Senescence Up (SenUp)," "Senescence Growth Arrest (SenGA)," "Inflammatory SASP (iSASP)," "Senescent Cell Anti-Apoptosis Pathways (SCAPs)," and "IFN-SASP" (Fig. 1D, Supplementary Table 3).

GSEA analysis was performed using the MGUS and SMM vs. healthy PC differential expression results. MGUS PCs exhibited significant enrichment of all custom gene sets (Fig. 1E; *q* value < 0.25). ssGSEA confirmed that enrichment for these gene sets was distributed throughout the MGUS cohort (Fig. 1F; Supplementary Fig. 2). SMM PCs also exhibited significant enrichment of "SenUp," "SCAPs," "SenGA," and "IFN-SASP," there were no significant differences in enrichment of these gene sets between MGUS and SMM PCs (Supplementary Fig. 3). However, SMM PCs did not show enrichment for "iSASP" compared to healthy PCs (Fig. 1E). This preferential enrichment of the "IFN-SASP" and absence of the "iSASP" enrichment is consistent with a transition to a late-senescence SASP phenotype. Using ssGSEA scores for "IFN-SASP" and "iSASP," we calculated the "IFN-SASP"/"iSASP" enrichment ratios for each normal, MGUS or SMM sample. The SMM samples exhibited a significant increase in the "IFN-SASP"/"iSASP" enrichment ratio compared to normal, with a trend for enrichment compared to MGUS (Fig. 1G). These data support that senescence genes are enriched in both MGUS and SMM PCs, with the inflammatory SASP being restricted to MGUS, and SMM patient PCs exhibiting a primarily IFN-SASP, consistent with late-senescence.

Cytologic features of senescence in MGUS PCs

We next investigated senescence cytologic features in MGUS, SMM, or newly diagnosed multiple myeloma (NDMM) PCs (Supplementary Table 4). Since MGUS and SMM PCs are non/low proliferative, we turned to additional senescence features beyond growth arrest. Senescence-associated distension of alpha-satellites (SADS) has previously been demonstrated as a cytologic feature of

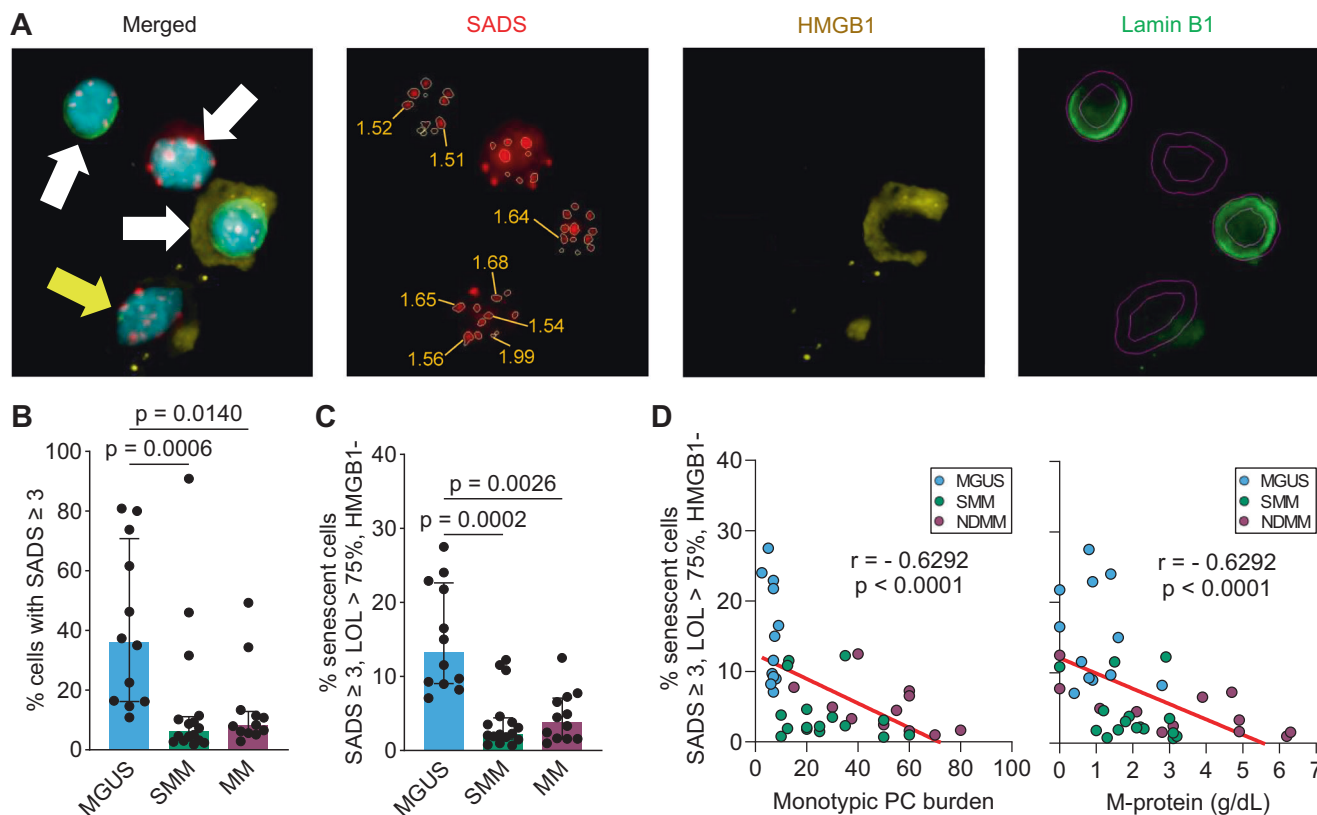


Fig. 2 Senescence cytologic features in MGUS, SMM, and NDMM patient PCs. **A** Representative images of cells stained for DAPI (cyan), CENPB (centromeres—red), HMGB1 (yellow), and LaminB1 (green). Yellow arrow indicates a cell considered senescent, based on the number of senescence-associated distension of alpha-satellite (SADS) per nucleus (three or more), loss of HMGB1 (LoH), and loss of LaminB1 (LoL). White arrows indicate non-senescent cells, defined as cells with less than three SADS per nucleus, presence of HMGB1, and/or presence of LaminB1. Red numbers indicate the calculation of the major axis length / minor axis length ratio in distended centromeres. **B** MGUS patient PCs exhibited a significant increase in the percentage of cells positive for three or more SADS per nucleus compared to SMM and MM. Bars represent medians with interquartile ranges. p values were calculated using the Kruskal-Wallis test followed by Dunn's multiple comparisons test. **C** When requiring LoH and LoL in addition to SADS to define senescence, the difference between MGUS and MM becomes more significant. Bars represent medians with interquartile ranges. p values were calculated using the Kruskal-Wallis test followed by Dunn's multiple comparisons test. **D** Significant inverse correlations between the percentage of senescent PCs and monoclonal PC (PC) burden or M-protein levels were observed. r and p values were calculated using the Spearman correlation test.

senescence [30, 31]. MGUS PCs exhibited a significant increase in the percentage of cells positive for ≥ 3 SADS per nucleus compared to SMM and MM (Fig. 2A, B). The difference between MGUS and SMM or MM became more significant when we applied the additional requirement of loss of LaminB1 and HMGB1 (Fig. 2A, C), two well-characterized senescence features [32, 33]. PCs that were positive for ≥ 3 SADS and loss of LaminB1/HMGB1 exhibited significantly increased nuclear size, consistent with senescence [34] (Supplemental Fig. 4).

Importantly, we found that the percentage of senescent PCs (≥ 3 SADS and loss of LaminB1/HMGB1) inversely correlated with monoclonal PC burden assessed by clinical flow and quantifiable M-spike (Fig. 2D). These results agree with a physiological role of senescence to prevent tumor progression in MM [12]. The percentage of senescent PCs did not correlate significantly with patient age, sex, or high-risk cytogenetic status, nor with hyperdiploidy.

Senescent PC burden correlates with senescence in the bone marrow microenvironment (BMME)

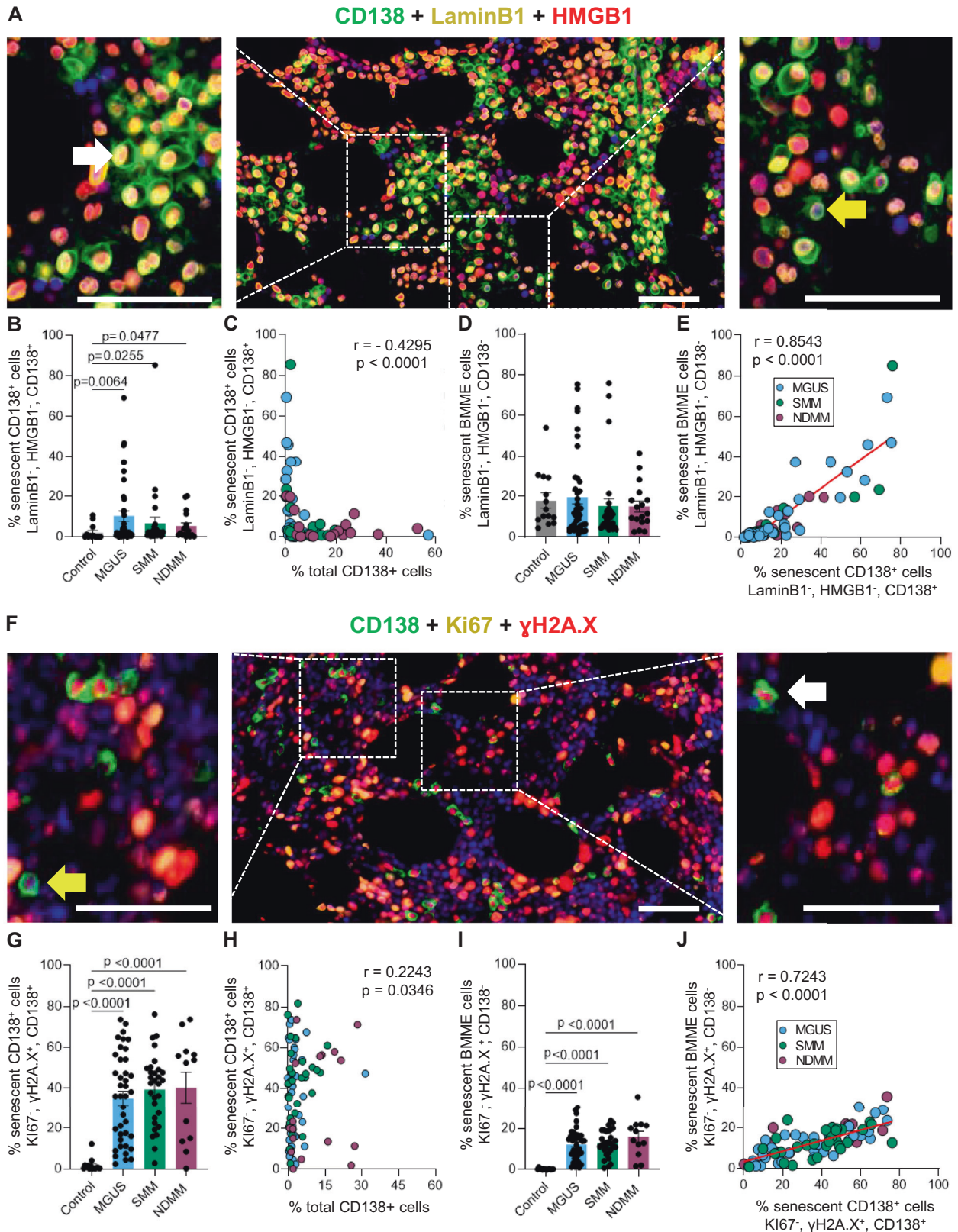
We next used diagnostic bone biopsies from a separate cohort of normal donors and patients with MGUS, SMM, or NDMM (Supplemental Table 5) to evaluate PC senescence within the intact BMME. PCs were detected via CD138 immunostaining in combination with immunostaining for LaminB1 and HMGB1

[32, 33] to evaluate senescence. Nucleated cells within the full bone biopsies were classified as CD138⁺ PCs vs. BMME (CD138⁻ nucleated cells). Senescent cells were defined as negative for both LaminB1 and HMGB1, and non-senescent cells as positive for both markers (Fig. 3A).

Quantification of PC burden in patient biopsies revealed a strong correlation of CD138⁺ PCs and the clinical histopathological assessment of tumor burden (Supplemental Fig. 5A), supporting the validity of our PC quantification. The percentage of senescent PCs was significantly increased in MGUS, SMM and NDMM biopsies compared to age-matched healthy donors (Fig. 3B). Of interest, PC senescence inversely correlated with total PC burden (Fig. 3C), consistent with our observations in isolated PCs (Fig. 2) and the established role for senescence in protecting against tumorigenesis.

In contrast to PCs, BMME senescence was not different between healthy donor and patient biopsies (Fig. 3D). There was no significant correlation between total senescent cell burden and donor/patient age (Supplemental Fig. 5B). However, PC senescence positively correlated with BMME senescence across patient biopsies (Fig. 3E), consistent with paracrine senescence.

To validate the relationship between the clonal PCs and senescent BMME we turned to additional senescence markers. Persistent DNA damage signaling in growth-arrested cells is a defining feature of senescence [35], and the DNA damage marker



phospho- γ H2AX (γ H2AX) is commonly assessed together with the proliferation marker Ki67 to identify senescent cells in tissue sections. We combined these markers with CD138 immunostaining; PCs or BMME were defined as senescent based on positivity

for γ H2AX and negativity for Ki67; non-senescent PCs or BMME were defined as all other cells (Fig. 3F).

Consistent with our LaminB1/HMGB1 analysis, we found a strong correlation between CD138⁺ PCs and the clinical

Fig. 3 **Histological senescence analysis of diagnostic bone marrow biopsies from patients with MGUS, SMM, or newly diagnosed MM (NDMM).** **A** Representative images of a triple immunostaining for CD138 (green), LaminB1 (yellow), and HMGB1 (red). The yellow arrow indicates a senescent PC, defined as CD138⁺, LaminB1⁻, and HMGB1⁻. The white arrow indicates a non-senescent PC, defined as CD138⁺, LaminB1⁺, and/or HMGB1⁺. **B** Senescent (S⁺, LaminB1⁻, HMGB1⁻) PCs (CD138⁺) were observed across healthy (Control), MGUS, SMM, and NDMM biopsies. **C** Significant inverse correlation between the percentage of senescent PCs (defined by no LaminB1/HMGB1) and PC (PC) burden was observed by Spearman correlation test. **D** Senescent (S⁺, LaminB1⁻, HMGB1⁻) bone marrow microenvironment cells (BMME, CD138⁻ cells) were observed across healthy (Control) MGUS, SMM, and NDMM biopsies. **E** The burden of senescent PCs significantly correlated with the percentage of senescent BMME across groups as measured by the Spearman correlation test. **F** Representative images of a triple immunostaining for CD138 (green), Ki67 (yellow), and γ H2A.X (red). The yellow arrow indicates a senescent PC, defined as CD138⁺, Ki67⁻, and γ H2A.X⁺. The white arrow indicates a non-senescent PC, defined as CD138⁺, Ki67⁺, and/or γ H2A.X⁻. **G** Senescent (S⁺, Ki67⁻, γ H2A.X⁺) PCs (CD138⁺) were observed across healthy (Control), MGUS, SMM, and NDMM biopsies. **H** Significant positive correlation between the percentage of senescent PCs (defined by Ki67⁻, γ H2A.X⁺) and PC (PC) burden was observed by Spearman correlation test. **I** Senescent (S⁺, Ki67⁻, γ H2A.X⁺) bone marrow microenvironment cells (BMME, CD138⁻ cells) were observed across healthy (Control), MGUS, SMM, and NDMM biopsies. **J** The burden of senescent PCs was significantly correlated with the percentage of senescent BMME across groups as measured by the Spearman correlation test.

histopathological assessments of tumor burden (Supplemental Fig. 5C), though consistently lower, possibly due to the specific antigen retrieval methods or variation across sections. Again, there was no significant correlation between total senescent cell burden and donor/patient age (Supplemental Fig. 5D).

Senescent PCs (Fig. 3G) were significantly increased in MGUS, SMM, and NDMM biopsies compared to healthy donors; there were no significant differences in senescent PCs across MGUS, SMM, or NDMM biopsies. PC senescence burden defined by γ H2AX/Ki67 was increased (Fig. 3G) compared to senescence defined by LaminB1/HMGB1 (Fig. 3B), and senescent PCs significantly correlated with total PC burden (Fig. 3H). These discrepancies suggests that the γ H2AX⁺/Ki67⁻ phenotype in clonal PCs may reflect genomic instability rather than senescence. The percentage of γ H2AX⁺/Ki67⁻ BMME was significantly increased in MGUS, SMM, and NDMM patient biopsies compared to healthy donors (Fig. 3I). Interestingly, γ H2AX⁺/Ki67⁻ PCs strongly correlated with senescent BMME in patient biopsies, consistent with clonal PCs being associated with paracrine senescence (Fig. 3J). Overall, these two independent analyses reveal the strong relationship between senescence and oncogenic stress in PCs and BMME senescence.

Spatial analysis reveals differential paracrine senescence in stable disease

Next, we stratified MGUS and SMM biopsies into stable or progressing disease based on the clinical diagnosis of MM ≤ 10 y or 5 y of sampling, respectively. These cut-offs were based on the risk for progression following diagnosis, with MGUS patients exhibiting a consistent risk of progression (1%/y) whereas SMM patients have significantly greater risk of progression ≤ 5 y (10%/y in the first 5 y, followed by 3%/y) [5]. To investigate the local neighborhoods around senescent and non-senescent PCs, we evaluated the cellular composition $\leq 25 \mu\text{m}$ of PCs in triplex immunostainings for CD138, LaminB1, and HMGB1, as shown in the digital spatial map of Fig. 4A. First, we evaluated the ratio of neighboring PCs to BMME around CD138⁺ senescent and non-PCs. As expected, the neighboring PC:BMME ratio was significantly increased in NDMM compared to stable or progressing MGUS and stable SMM, consistent with proliferative PC disease in MM (Fig. 4B).

Density heatmaps showed increased senescent BMME in stable MGUS and SMM patients, compared to those with progressing disease; moreover, the spatial distribution of senescent BMME showed high-density spots, supporting a role for paracrine senescence within the proximate *milieu* (Fig. 4C). The neighboring BMME compartment was further assessed for the ratio of proximate senescent vs. non-senescent BMME. In stable MGUS and SMM biopsies, there was a significant increase in proximate senescent BMME to senescent PCs as compared to non-senescent PCs (Fig. 4D). Surprisingly, however, the progressing MGUS and

SMM, as well as the NDMM biopsies, did not show significant increases in proximate senescent BMME to senescent PCs (Fig. 4D). Further evaluation of MGUS and SMM biopsies from progressing patients revealed that the average percentage of non-senescent BMME $\leq 25 \mu\text{m}$ of senescent PCs negatively correlated with years to progression, showing that patients with highest percentage of non-senescent BMME proximate to senescent PCs progressed the most quickly (Fig. 4E).

SASP evaluation in stable vs. progressing MGUS and SMM

Given that paracrine senescence is activated via the SASP [36], along with the differences in "iSASP" gene enrichment in MGUS and SMM PCs (Fig. 1), we tested whether patients with stable MGUS or SMM exhibited differences in SASP factors and whether these were associated with progression. Stable MGUS and SMM patients were identified based on the lack of progression to MM ≤ 10 y or 5 y, respectively, following sample collection (Supplemental Table 6). Peripheral plasma was assessed for SASP factors that were previously tested for associations with frailty [37], as well as for cell-free mitochondrial (MT)-DNA which has been shown to activate the inflammatory SASP [38] (Fig. 5A). Of the thirteen SASP factors measured, cell-free MT-DNA, and IL-7 were significantly elevated in stable MGUS, while osteopontin (OPN), GDF15, and TNF- α were significantly increased in stable SMM (Fig. 5A). Of interest, GDF-15 and OPN are induced by IFN signaling, consistent with a preferential late senescence "IFN-SASP" enrichment in SMM (Fig. 1).

Subsequent ranking and analysis of the top 50th percentile for each factor revealed skewing of certain markers towards stable MGUS and others towards stable SMM (Fig. 5B). Grouping the factors that skewed towards stable MGUS (odds ratio ≥ 1.5) vs. the factors that skewed towards stable SMM (odds ratio ≤ 0.5) allowed us to generate composite SASP scores specific to stable MGUS or SMM, respectively (Fig. 5C, D). The MGUS SASP score discriminated stable MGUS from healthy age-matched donors, while the SMM SASP score tended to be increased in SMM compared to healthy donors. By subtracting the SMM-SASP score from the MGUS-SASP, we created the MGUS-SMM SASP score, which further discriminated between stable MGUS and healthy donors (Fig. 5E). None of the identified peripheral SASP factors were significantly different by gene expression analysis of MGUS and SMM PCs (Supplemental Fig. 2), suggesting they reflect paracrine senescence rather than direct products of the pre-malignant PCs.

We next evaluated the composite stable MGUS-SMM SASP scores across MGUS and SMM patients who progressed and NDMM. In this larger dataset (Fig. 6A), the MGUS-SMM SASP composite score demonstrated that stable MGUS still showed significant increase compared to stable SMM (Fig. 6B), with the PC burden inversely correlating with the stable MGUS-SMM SASP score in stable patients (Fig. 6C). Stable SMM also exhibited a significant decrease in the stable MGUS-SASP score compared to

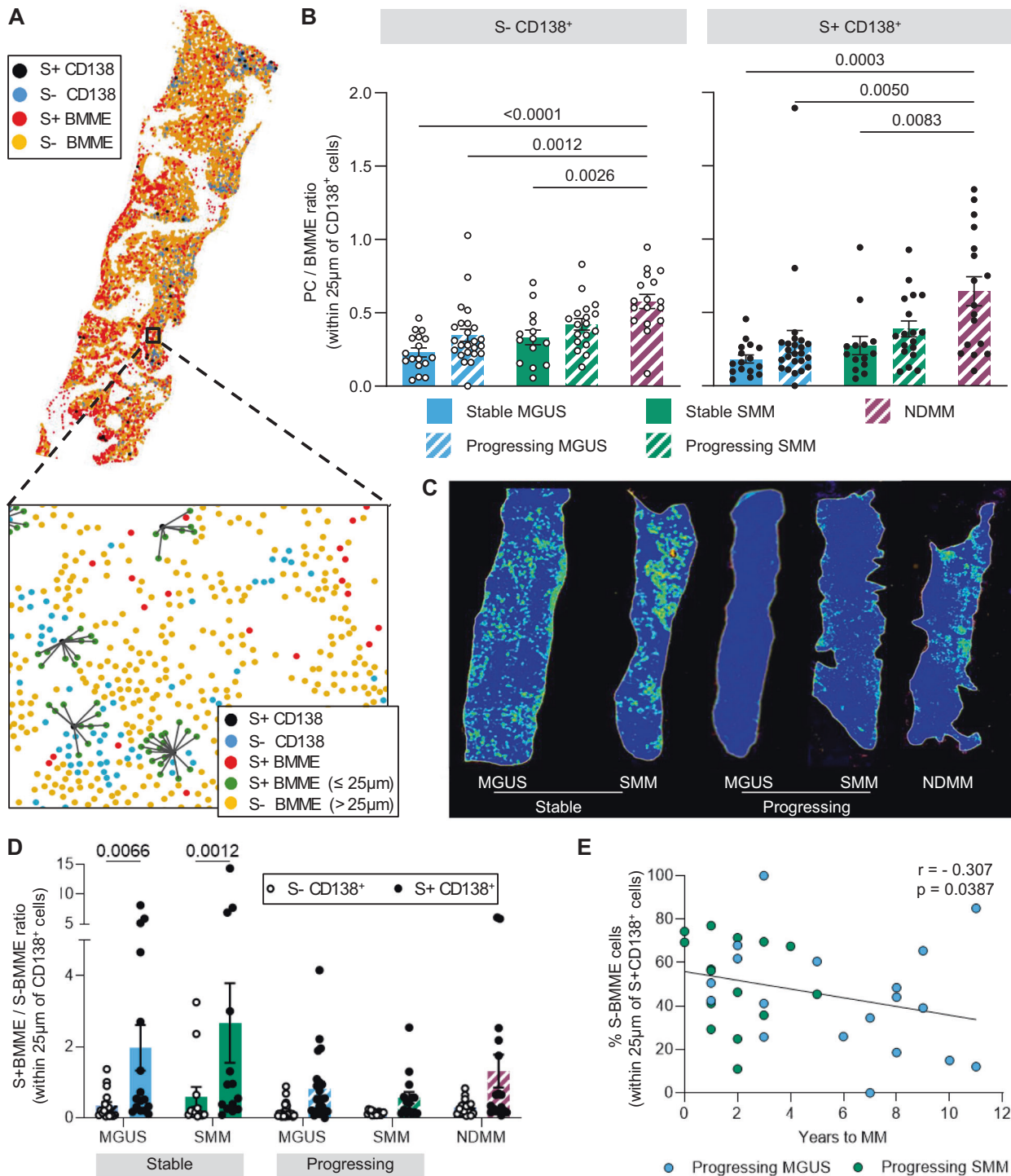


Fig. 4 Spatial analysis of senescent and non-senescent cells in MGUS, SMM and newly diagnosed MM (NDMM) patient biopsies stratified by disease progression status. **A** Representative schematic of the spatial histological assessment in trephine bone biopsy. Each dot represents a cell, colored according to cell type, senescence status, and proximity to senescent PC. **B** Ratio of PCs (PC; CD138⁺) to bone marrow microenvironment cells (BMME; CD138⁺) neighboring senescent (S+, white dots) or non-senescent (S-, black dots) PCs. PCs surrounding both senescent and non-senescent PCs were increased in NDMM compared to stable or progressing MGUS and stable SMM. **C** Density heatmaps showed localized increases in senescent cells in stable MGUS and SMM patients, as compared to progressing or NDMM patients. **D** Comparing the ratio of senescent to non-senescent BMME neighboring non-senescent PCs (white dots) vs. senescent PCs (black dots) revealed significant enrichment of senescent BMME in the proximity of senescent PCs in stable MGUS and SMM biopsies, but not in progressing disease or NDMM biopsies. **E** The negative correlation between the average percentage of non-senescent BMME within 25 μ m of senescent PCs and years to progression to MM in MGUS and SMM patients was significant, as measured by the Spearman correlation test.

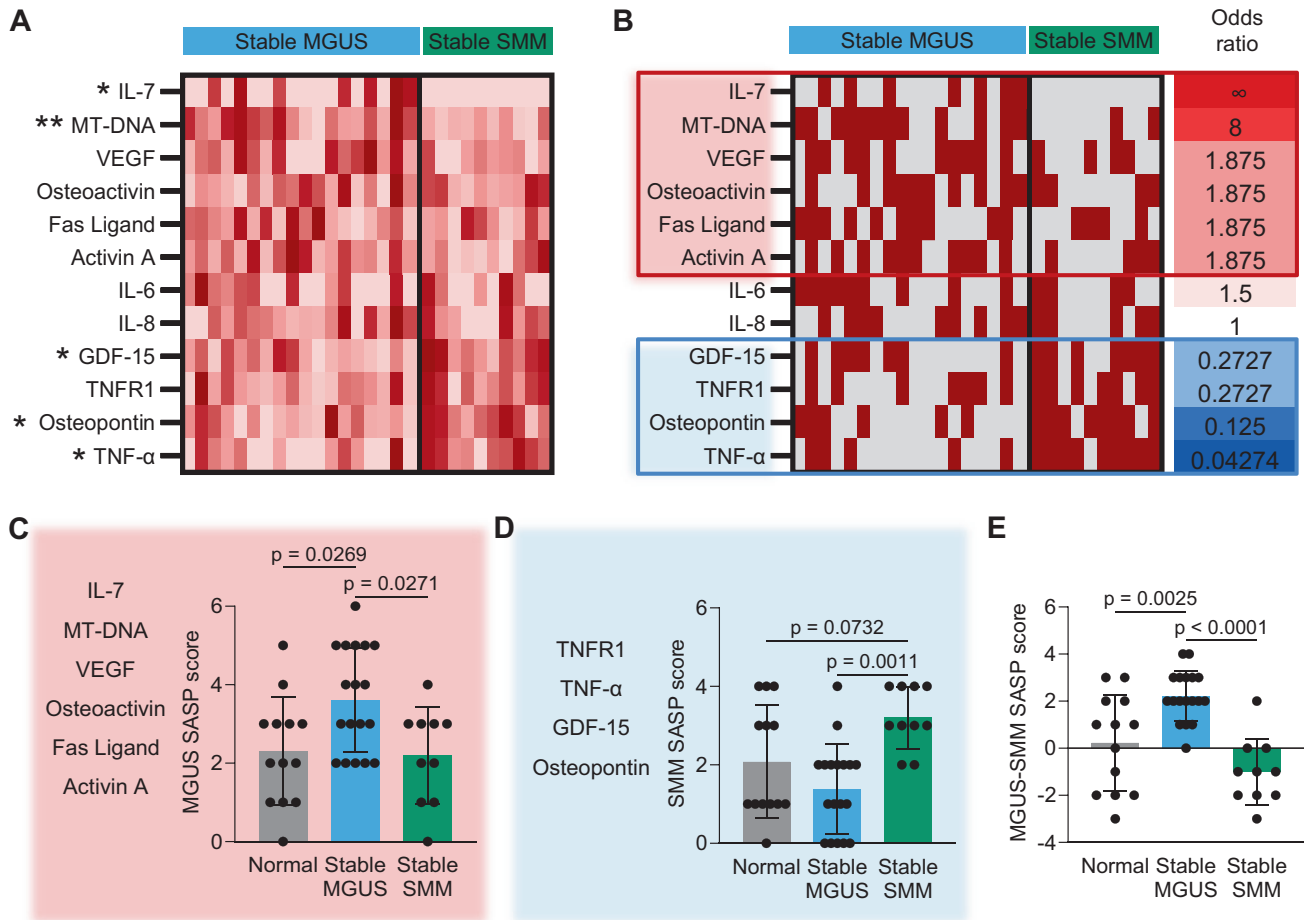


Fig. 5 SASP factor analysis of peripheral plasma isolated from stable MGUS and SMM patients. **A** Peripheral plasma from stable MGUS and SMM patients was assessed for SASP factors associated with frailty, as well as cell-free mitochondrial (MT)-DNA. Heatmap shows the patients ranked per SASP factor. Among the twelve measured SASP factors, MT-DNA, and IL-7 were significantly elevated in stable MGUS, while osteopontin (OPN), GDF15, and TNF- α were significantly increased in stable SMM. Asterisks indicate a significant difference in the plasma concentration of a marker (* $p < 0.05$, ** $p < 0.01$) between stable MGUS and stable SMM patients, as measured by the Mann-Whitney test. **B** Analysis of the top 50th percentile (in maroon) for each factor revealed certain markers skewed towards stable MGUS and others towards stable SMM, indicating distinct SASP profiles in these conditions. **C** A composite SASP score were generated for stable MGUS based on factors that skewed towards MGUS vs. SMM (odds ratio greater than 1.5). **D** Composite SASP score generated for stable SMM based on factors that skewed towards SMM vs. MGUS (odds ratio lower than 0.5). **E** MGUS-SMM SASP composite score, calculated by subtracting the SMM SASP score from the MGUS SASP score. Bars represent means with standard deviations (SD). p-values were calculated using the one-way ANOVA test followed by Tukey's multiple comparisons test.

SMM patients that progressed ≤ 5 y. The correlation of stable MGUS-SMM SASP score with PC burden was absent in progressing MGUS, SMM, and NDMM patient samples. Together with our spatial analyses, these data suggest that failure of SASP-induced paracrine senescence is key to disease progression.

DISCUSSION

In this study, we comprehensively evaluated MGUS, SMM, and MM patient samples to demonstrate that senescence and SASP features are present in precursor monoclonal gammopathies. Our analyses showed that senescence features were independent of chronological age. Further, SASP scores and paracrine senescence appeared most prominent in patients with stable disease. These data generated entirely with clinical samples demonstrate the crucial role of senescence in preventing tumorigenesis within the context of a senescence-responsive microenvironment.

Although senescence was originally characterized as replicative senescence in proliferative cells [39], it has now been established that terminally differentiated, non-proliferative cells can also

become senescent following exposure to stressors [40, 41]. Thus, beyond growth arrest, defining senescence requires evaluation of a combination of features, which is further complicated by the fact that senescence phenotypes may be variable across cell lineages and specific stress responses. We carefully considered current guidance on senescent cell characterization [42] to evaluate senescent features in MGUS and SMM PCs and biopsies.

Differentiated PCs, along with pre-malignant PCs in MGUS and SMM, exhibit no/low proliferative activity. Growth arrest in these populations was supported by increased expression of the cell cycle checkpoint inhibitor *CDKN1A* (p21), along with enrichment of other genes associated with senescence growth arrest, compared to normal PCs (Fig. 1). We further used a combination of cytologic features to classify PCs or their proximate BMME as senescent or non-senescent. This included evaluation of SADS and loss of LaminB1/HMGB1 in enriched PCs (Fig. 2), as well as loss of LaminB1/HMGB1 or the presence of γ H2AX⁺/Ki67⁻ cells in bone biopsies (Figs. 3, 4). These separate analyses of independent patient cohorts revealed increased senescence in MGUS PCs compared to those from SMM or MM (Fig. 2), as well as paracrine senescence in MGUS and SMM that was associated with stable

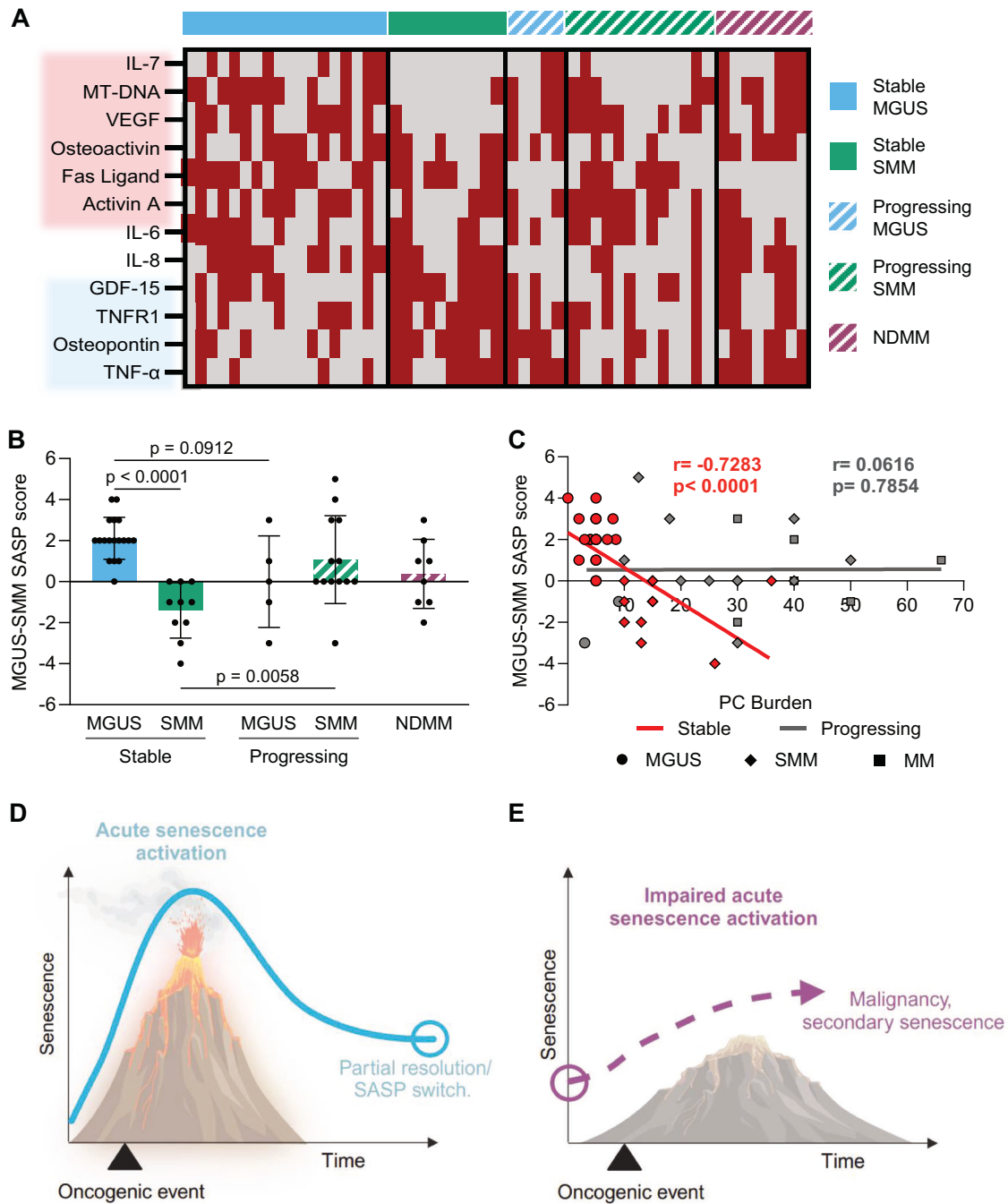


Fig. 6 Evaluation of stable MGUS and SMM SASP composite scores across patients that progressed to MM and NDMM patients. **A** Dataset was expanded from one presented in Fig. 5B. Redistribution of patients according to the 50th percentile (top 50th percentile in maroon, lower 50th percentile in gray) showed that the SASP markers that constitute the stable MGUS composite score (highlighted in red) and the stable SMM composite score (highlighted in blue) were still enriched in their respective sets of patients. **B** The analysis of the stable MGUS-SMM SASP composite score across the groups still showed significant enrichment in stable MGUS patients compared to stable SMM patients. Bars represent means with SD. p-values were calculated using the one-way ANOVA test followed by Tukey's multiple comparisons test. **C** A significant inverse correlation between stable MGUS-SMM SASP score and PC (PC) burden was observed in stable patients, but no correlation was identified in progressing patients. r and p-values were calculated using the Spearman correlation test. **D, E** Schematic representation of time-course of senescence activation and clearing in stable vs. progressing MGUS/SMM conditions. **D** In patients with stable MGUS/SMM, oncogenic activation induces an acute cellular and paracrine senescence response that is partially cleared over time; a high burden of senescence cells remains upon immune clearing (blue circle), which may contribute to accelerated aging at expense of tumor inhibition in stable patients. **E** Patients with chronically increased senescent burden prior to oncogenic activation (purple circle) fail to activate cellular and paracrine senescence responses, which result in progression to MM.

disease (Fig. 4). The paracrine senescence in stable disease was further supported by evaluation of the SASP factors in MGUS, SMM, and MM plasma, which showed distinct SASP profiles in stable MGUS vs. stable SMM (Figs. 5, 6), consistent with altered SASP phenotypes in gene expression analyses (Fig. 1).

Our data support that the ability of senescence to protect against tumorigenesis is linked to the SASP and paracrine senescence. The SASP is crucial for driving immune responses to clear damaged, potentially malignant cells, including senescent cells. Two recent reports demonstrated that senescence in malignant cells drives CD8 T cell anti-tumor immunity [43, 44]. Together with our data (Fig. 6), this suggests that a blunted SASP promotes tumor progression by failing to trigger immune clearance of pre-malignant/malignant cells. In addition to immune activation, the SASP drives paracrine senescence to reinforce growth arrest. Accordingly, we found a significant decrease in senescent BMME proximate to senescent PCs. Moreover, the percent of non-senescent BMME proximate to senescent PCs inversely correlated with time to progression in MGUS and SMM (Fig. 4).

While our *ex vivo* PC senescence analysis did not discern between clonal and polyclonal PCs, we may glean insights from sample-specific clinical data. For one MGUS sample, clinical flow showed <5% polyclonal PCs relative to total PCs, suggesting that the 16% senescence detected in sorted PCs reflects clonal PC senescence. In contrast, another MGUS sample had no detectable clonal PCs; therefore, 24% senescence must represent polyclonal PC senescence. These two extremes suggest that both clonal and polyclonal PCs exhibit senescence in MGUS, with non-clonal PCs possibly responding to paracrine senescence signals and only a subset of clonal PCs undergoing senescence. In turn, non-senescent clonal cells may sustain low-level proliferation that may eventually develop into stable SMM; over time, growth arrested cells may be diluted, reducing the percentage of senescent PCs. Despite this decrease, similar senescence gene expression between MGUS and SMM PCs implies that late-senescent SMM PCs with higher senescence gene expression may mask overall differences in senescent cell number in bulk RNA analyses.

The altered SASP and lack of paracrine senescence in progressing MGUS and SMM suggest either (1) impaired senescence/SASP activation in the pre-malignant PCs or (2) reduced BMME responsiveness to paracrine SASP signals, leading to weakened immune responses to clonal PCs. While mutations to genes such as *TP53* in clonal PCs could impair the commitment to senescence growth arrest and attenuate the SASP, *TP53* mutations are not usually present in MGUS and SMM PCs [45, 46] but rather are acquired as secondary genetic events. [33] Further, our reanalysis of data published by Sun et al. [47] found no differences in senescence gene sets between PCs from stable vs. progressing MGUS patients (data not shown). In contrast, there is strong evidence for the latter, with age and obesity—two conditions associated with senescent cell accumulation [20, 21], being risk factors for MGUS and SMM incidence and progression [17–19]. Thus, chronic senescence could impair the ability of the BMME and immune microenvironment to respond to acute oncogenic stress-induced senescence, leading to disease progression (Fig. 6F, G).

Indeed, senescence in the microenvironment has been shown to promote tumor growth and metastasis, with IL6 and p38 MAPK signaling playing important roles [48, 49]. Our analysis of bone biopsies showed no increase in the BMME senescence burden in progressing patients; instead, BMME senescence correlated with PC senescence and was higher in the stable patients. However, oncogenic stress-induced paracrine senescence may have masked any differences in baseline chronic senescence in progressing patients. Alternatively, evaluation of chronic senescence may be improved by assessment of specific stromal populations.

This raises important questions regarding the potential use of senotherapeutic drugs in pre-malignant conditions. Our analyses suggest that only a subset of clonal and polyclonal PCs is senescent, and these cells drive the anti-tumor effects. Therefore, what is the impact of ablating these senescent cells *via* senolytic drugs on the anti-tumor immune response? To date, senescent cell ablation has not been reported to increase tumor incidence in mouse models [14, 15]; it is possible that pre-tumor cells are also ablated in these models. Alternatively, the positive effects of reducing senescent cell burden to mitigate inflammaging could enhance anti-tumor immune function. This is supported by a retrospective study demonstrating that metformin, which can act as a senomorphic through inhibition of the SASP [22], prevented MM progression in diabetic MGUS patients [23, 24].

Further research is needed to discriminate between these possibilities, and to determine whether the impact of senotherapeutics may be context dependent, such that with chronic senescence, these drugs may alleviate immune tolerance and allow enhanced anti-tumor effect, whereas in an immune responsive microenvironment, senotherapeutics may have limited efficacy. In this case, immune clearance of pre-malignant cells may be enhanced *via* drugs that reinforce senescence. We propose that failure of paracrine senescence or impaired acute senescence-induced CD8 T cell activation [43, 44] may serve as indicators of chronic senescent cell burden to identify patients most likely to benefit from senotherapeutics in the setting of pre-malignancy.

These studies may help explain the decreased overall survival in patients with monoclonal gammopathies. MGUS without progression to MM have been found to die or exhibit morbidity from cardiovascular or neurological diseases at earlier ages than patients without M-spikes [50–52]. Indeed, patients with stable MGUS and SMM are at increased risk for osteoporosis and fracture unrelated to osteolytic cancer-bone disease [53]. This leads to the provocative question of whether enhanced anti-tumor senescence signaling in these stable MGUS/SMM patients comes at the expense of accelerated physiological aging. This possibility is highly reminiscent of the findings that defects in transcription-coupled nucleotide excision repair, in which low-level DNA damage activates cell stress responses to protect against malignancy, drives the progeroid conditions, Cockayne's Syndrome and Trichothiodystrophy [54]. It has been postulated by Dr. Hoeijmakers and others that these DNA damage responses trigger inflammatory signaling and altered endocrine signaling to drive survival, rather than preserving normal cellular functionality, leading to aging changes [55].

Overall, our results raise the prospect of using SASP and paracrine senescence markers to predict the risk for patients with pre-malignant conditions to progress to malignancy. Current risk-stratification tools show limited efficacy, especially for SMM. In this context, SASP profiling may arise as a novel prognostic biomarker which may increase our ability to identify MGUS and SMM patients at highest risk for progression who may benefit from early intervention. These SASP and paracrine senescence clinical analyses may also facilitate the identification of patients who would benefit from serotherapeutic treatment as these agents move into clinical trials for malignant disease.

DATA AVAILABILITY

The microarray dataset analyzed for the characterization of senescence phenotypes in healthy, MGUS, and SMM patients is available in the Gene Expression Omnibus (GEO) database under accession number GSE5900. The microarray and bulk RNA sequencing datasets used as references for cellular senescence in our strategy to develop senescence phenotyping gene sets are available in the GEO database under accession numbers GSE66236 and GSE109700. The senescence phenotyping gene sets are described in Supplemental Table 3. The full results of the iPathwayGuide Pathway Analysis are presented in Supplemental Table 2, and the results of the Gene Set Enrichment Analysis (GSEA) using our senescence phenotyping gene sets are

described in Supplemental Table 7. All data generated during this study are included in this published article and its supplementary information files.

REFERENCES

- American Cancer Society. Cancer Facts & Figures 2024. Atlanta: American Cancer Society. 2024.
- Landgren O, Kyle RA, Pfeiffer RM, Katzmann JA, Caporaso NE, Hayes RB, et al. Monoclonal gammopathy of undetermined significance (MGUS) consistently precedes multiple myeloma: a prospective study. *Blood*. 2009;113:5412–7.
- Weiss BM, Abadie J, Verma P, Howard RS, Kuehl WM. A monoclonal gammopathy precedes multiple myeloma in most patients. *Blood*. 2009;113:5418–22.
- Kyle RA, Durie BG, Rajkumar SV, Landgren O, Blade J, Merlini G, et al. Monoclonal gammopathy of undetermined significance (MGUS) and smoldering (asymptomatic) multiple myeloma: IMWG consensus perspectives risk factors for progression and guidelines for monitoring and management. *Leukemia*. 2010;24:1121–7.
- Kyle RA, Remstein ED, Therneau TM, Dispenzieri A, Kurtin PJ, Hodnefeld JM, et al. Clinical course and prognosis of smoldering (asymptomatic) multiple myeloma. *N Engl J Med*. 2007;356:2582–90.
- Cowan A, Ferrari F, Freeman SS, Redd R, El-Khoury H, Perry J, et al. Personalised progression prediction in patients with monoclonal gammopathy of undetermined significance or smoldering multiple myeloma (PANGEA): a retrospective, multicohort study. *Lancet Haematol*. 2023;10:e203–e212.
- Van de Wyngaert Z, Boyle EM. The PANGEA model: catching the drift from precursor conditions to myeloma in individual patients. *Lancet Haematol*. 2023;10:e162–e163.
- Fonseca R, Bailey RJ, Ahmann GJ, Rajkumar SV, Hoyer JD, Lust JA, et al. Genomic abnormalities in monoclonal gammopathy of undetermined significance. *Blood*. 2002;100:1417–24.
- Kaufmann H, Ackermann J, Baldia C, Nösslinger T, Wieser R, Seidl S, et al. Both IGH translocations and chromosome 13q deletions are early events in monoclonal gammopathy of undetermined significance and do not evolve during transition to multiple myeloma. *Leukemia*. 2004;18:1879–82.
- Chng WJ, Van Wier SA, Ahmann GJ, Winkler JM, Jalal SM, Bergsagel PL, et al. A validated FISH trisomy index demonstrates the hyperdiploid and non-hyperdiploid dichotomy in MGUS. *Blood*. 2005;106:2156–61.
- Abbas T, Dutta A. p21 in cancer: intricate networks and multiple activities. *Nat Rev Cancer*. 2009;9:400–14.
- LaPak KM, Burd CE. The molecular balancing act of p16(INK4a) in cancer and aging. *Mol Cancer Res*. 2014;12:167–83.
- Burd CE, Sorrentino JA, Clark KS, Darr DB, Krishnamurthy J, Deal AM, et al. Monitoring tumorigenesis and senescence in vivo with a p16INK4a-luciferase model. *Cell*. 2013;152:340–51.
- Burd CE, Sorrentino JA, Clark KS, Darr DB, Krishnamurthy J, Deal AM, et al. Naturally occurring p16(INK4a)-positive cells shorten healthy lifespan. *Nature*. 2016;530:184–9.
- Xu M, Pirtskhalava T, Farr JN, Weigand BM, Palmer AK, Weivoda MM, et al. Senolytics improve physical function and increase lifespan in old age. *Nature Med*. 2018;24:1246–56.
- Krtolica A, Parrinello S, Lockett S, Desprez PY, Campisi J. Senescent fibroblasts promote epithelial cell growth and tumorigenesis: a link between cancer and aging. *Proc Natl Acad Sci USA*. 2001;98:12072–7.
- Kyle RA, Therneau TM, Rajkumar SV, Larson DR, Plevak MF, Offord JR, et al. Prevalence of monoclonal gammopathy of undetermined significance. *N Engl J Med*. 2006;354:1362–9.
- Turesson I, Velez R, Kristinsson SY, Landgren O. Patterns of multiple myeloma during the past 5 decades: stable incidence rates for all age groups in the population but rapidly changing age distribution in the clinic. *Mayo Clin Proc*. 2010;85:225–30.
- Thordardottir M, Lindqvist EK, Lund SH, Costello R, Burton D, Korde N, et al. Obesity and risk of monoclonal gammopathy of undetermined significance and progression to multiple myeloma: a population-based study. *Blood Adv*. 2017;1:2186–92.
- Campisi J. Senescent cells, tumor suppression, and organismal aging: good citizens, bad neighbors. *Cell*. 2005;120:513–22.
- Tchkonia T, Morbeck DE, Von Zglinicki T, Van Deursen J, Lustgarten J, Scrable H, et al. Fat tissue, aging, and cellular senescence. *Aging Cell*. 2010;9:667–84.
- Moiseeva O, Deschênes-Simard X, St-Germain E, Igelmann S, Huot G, Cadar AE, et al. Metformin inhibits the senescence-associated secretory phenotype by interfering with IKK/NF- κ B activation. *Aging Cell*. 2013;12:489–98.
- Chang SH, Luo S, O'Brian KK, Thomas TS, Colditz GA, Carlsson NP, et al. Association between metformin use and progression of monoclonal gammopathy of undetermined significance to multiple myeloma in US veterans with diabetes mellitus: a population-based retrospective cohort study. *Lancet Haematol*. 2015;2:e30–36.
- Boursi B, Mamtani R, Yang YX, Weiss BM. Impact of metformin on the progression of MGUS to multiple myeloma. *Leuk Lymphoma*. 2017;58:1265–7.
- Zhan F, Barlogie B, Arzoumanian V, Huang Y, Williams DR, Hollmig K, et al. Gene-expression signature of benign monoclonal gammopathy evident in multiple myeloma is linked to good prognosis. *Blood*. 2007;109:1692–1700.
- Saul D, Kosinsky RL, Atkinson EJ, Doolittle ML, Zhang X, LeBrasseur NK, et al. A new gene set identifies senescent cells and predicts senescence-associated pathways across tissues. *Nature Commun*. 2022;13: 4827.
- Oetjen KA, Lindblad KE, Goswami M, Gui G, Dagur PK, Lai C, et al. Human bone marrow assessment by single-cell RNA sequencing, mass cytometry, and flow cytometry. *JCI Insight*. 2018;3:e124928.
- Zhu Y, Tchkonia T, Pirtskhalava T, Gower AC, Ding H, Giorgadze N, et al. The Achilles' heel of senescent cells: from transcriptome to senolytic drugs. *Aging Cell*. 2015;14:644–58.
- De Cecco M, Ito T, Petrashen AP, Elias AE, Skvir NJ, Criscione SW, et al. L1 drives IFN in senescent cells and promotes age-associated inflammation. *Nature*. 2019;566:73–78.
- De Cecco M, Criscione SW, Peckham EJ, Hillenmeyer S, Hamm EA, Manivannan J, et al. Genomes of replicatively senescent cells undergo global epigenetic changes leading to gene silencing and activation of transposable elements. *Aging Cell*. 2013;12:247–56.
- Swanson EC, Manning B, Zhang H, Lawrence JB. Higher-order unfolding of satellite heterochromatin is a consistent and early event in cell senescence. *J Cell Biol*. 2013;203:929–42.
- Freund A, Laberge RM, Demaria M, Campisi J. Lamin B1 loss is a senescence-associated biomarker. *Mol Biol Cell*. 2012;23:2066–75.
- Davalos AR, Kawahara M, Malhotra GK, Schaub N, Huang J, Ved U, et al. p53-dependent release of Alarmin HMGB1 is a central mediator of senescent phenotypes. *J Cell Biol*. 2013;201:613–29.
- Mitsui Y, Schneider EL. Increased nuclear sizes in senescent human diploid fibroblast cultures. *Exp Cell Res*. 1976;100:147–52.
- Wang C, Jurk D, Maddick M, Nelson G, Martin-Ruiz C, Von Zglinicki T. DNA damage response and cellular senescence in tissues of aging mice. *Aging Cell*. 2009;8:311–23.
- Acosta JC, Banito A, Wuestefeld T, Georgilis A, Janich P, Morton JP, et al. A complex secretory program orchestrated by the inflammasome controls paracrine senescence. *Nat Cell Biol*. 2013;15:978–90.
- Schafer MJ, Zhang X, Kumar A, Atkinson EJ, Zhu Y, Jachim S, et al. The senescence-associated secretome as an indicator of age and medical risk. *JCI Insight*. 2020;5:e133668.
- Iske J, Seyda M, Heinbokel T, Maenosono R, Minami K, Nian Y, et al. Senolytics prevent mt-DNA-induced inflammation and promote the survival of aged organs following transplantation. *Nat Commun*. 2020;11: 4289.
- Hayflick L, Moorhead PS. The serial cultivation of human diploid cell strains. *Experimental Cell Res*. 1961;25:585–621.
- Jurk D, Wang C, Miwa S, Maddick M, Korolchuk V, Tzolou A, et al. Postmitotic neurons develop a p21-dependent senescence-like phenotype driven by a DNA damage response. *Aging Cell*. 2012;11:996–1004.
- Minamino T, Orimo M, Shimizu I, Kunieda T, Yokoyama M, Ito T, et al. A crucial role for adipose tissue p53 in the regulation of insulin resistance. *Nat Med*. 2009;15:1082–7.
- Suryadevara V, Hudgins AD, Rajesh A, Pappalardo A, Karpova A, Dey AK, et al. SenNet recommendations for detecting senescent cells in different tissues. *Nature Rev Mol Cell Biol*. 2024;25:1001–23.
- Chen H-A, Ho Y-J, Mezzadra R, Adrover JM, Smolkin R, Zhu C, et al. Senescence rewires microenvironment sensing to facilitate antitumor immunity. *Cancer Discov*. 2023;13:432–53.
- Marin I, Boix O, Garcia-Garjito A, Sirois I, Caballe A, Zarzuela E, et al. Cellular senescence is immunogenic and promotes antitumor immunity. *Cancer Discov*. 2023;13:410–31.
- Mikulasova A, Wardell CP, Murison A, Boyle EM, Jackson GH, Smetana J, et al. The spectrum of somatic mutations in monoclonal gammopathy of undetermined significance indicates a less complex genomic landscape than that in multiple myeloma. *Haematologica*. 2017;102:1617–25.
- Kuehl WM, Bergsagel PL. Multiple myeloma: evolving genetic events and host interactions. *Nature Rev Cancer*. 2002;2:175–87.
- Sun F, Cheng Y, Ying J, Mery D, Al Hadidi S, Wanchai V, et al. A gene signature can predict risk of MGUS progressing to multiple myeloma. *J Hematol Oncol*. 2023;16:70.
- Luo X, Fu Y, Loza AJ, Murali B, Leahy KM, Ruhland MK, et al. Stromal-initiated changes in the bone promote metastatic niche development. *Cell Rep*. 2016;14:82–92.
- Alimirah F, Pulido T, Valdovinos A, Alptekin S, Chang E, Jones E, et al. Cellular senescence promotes skin carcinogenesis through p38MAPK and p44/42MAPK signaling. *Cancer Res*. 2020;80:3606–19.

50. Kristinsson SY, Björkholm M, Andersson TM, Eloranta S, Dickman PW, Goldin LR, et al. Patterns of survival and causes of death following a diagnosis of monoclonal gammopathy of undetermined significance: a population-based study. *Haematologica*. 2009;94:1714–20.
51. Kyle RA, Larson DR, Therneau TM, Dispenzieri A, Kumar S, Cerhan JR, et al. Long-Term follow-up of monoclonal gammopathy of undetermined significance. *N Engl J Med*. 2018;378:241–9.
52. Schwartz B, Schou M, Ruberg FL, Rucker D, Choi J, Siddiqi O, et al. Cardiovascular morbidity in monoclonal gammopathy of undetermined significance. *CardioOncology*. 2022;4:313–22.
53. Melton LJ 3rd, Rajkumar SV, Khosla S, Achenbach SJ, Oberg AL, Kyle RA. Fracture risk in monoclonal gammopathy of undetermined significance. *J Bone Min Res*. 2004;19:25–30.
54. Hoeijmakers JHJ. DNA damage, aging, and cancer. *New Engl J Med*. 2009;361:1475–85.
55. Schumacher B, Pothof J, Vijg J, Hoeijmakers JHJ. The central role of DNA damage in the ageing process. *Nature*. 2021;592:695–703.

ACKNOWLEDGEMENTS

We thank Kaja Laursen for excellent technical help. This work has been supported by NIH (Onco-Aging Consortium, U01AG075227; Translational Geroscience Network, R33AG61456; R37AG13925), Hevolution Foundation (HF-GRO-23-1199148-3), Connor Fund, Robert J. and Theresa W. Ryan, Noaber Foundation, NEYE fonden, Carl and Ellen Hertz, Dr. Phil. Ranga Rask-Nielsen's Basic Research Fund, Dagmars Midelegat, Fraenkels Mindefond, Holms Mindelegat and the Danish Cancer Society.

AUTHOR CONTRIBUTIONS

Conceptualization of the project: GAB, MDC, MTD, TLA, MMW; Data collection and analysis: GAB, MDC, AJG, BMEM, FAM, MMW; Contribution of data/samples: MTG, MH, TL, NA, LBB, TK, MTD; Discussion and interpretation of results: GAB, MDC, AJG, NA, LBB, MX, AG, TT, JLK, TK, MTD, TLA, MMW; Drafting of manuscript: GAB, MDC, MMW; All authors reviewed the final manuscript.

COMPETING INTERESTS

TT and JLK have a financial interest related to this research, including patents and pending patents covering senolytic drugs and their uses held by Mayo Clinic. This research has been reviewed by the Mayo Clinic Conflict of Interest Review Board and was conducted in compliance with Mayo Clinic conflict of interest policies.

ETHICS APPROVAL AND CONSENT TO PARTICIPATE

All methods described in this manuscript were performed in accordance with the relevant guidelines and regulations. The human study protocols reported in this

manuscript were conducted in accordance with the Declaration of Helsinki. Patients who donated bone marrow aspiration samples and peripheral plasma provided written informed consent in accordance with the biobanking study protocol, which was approved by the Mayo Clinic Institutional Review Board under the number 521-93. Analyses of these samples was approved by the Mayo Clinic Institutional Review Board under the number 20-002263. Trephine iliac crest bone biopsies from MGUS, SMM, and NDMM patients were obtained from Danish pathological biobanks under approval from the Danish National Committee on Biomedical Research Ethics (S-20190110) and in compliance with the Declaration of Helsinki. All patients provided written informed consent. Bone biopsies from healthy individuals were included from a previous study approved by the Danish National Committee on Biomedical Research Ethics under protocol number 1-10-72-223-20, with informed consent obtained from all participants.

ADDITIONAL INFORMATION

Supplementary information The online version contains supplementary material available at <https://doi.org/10.1038/s41375-025-02572-z>.

Correspondence and requests for materials should be addressed to Thomas Levin Andersen or Megan M. Weivoda.

Reprints and permission information is available at <http://www.nature.com/reprints>

Publisher's note Springer Nature remains neutral with regard to jurisdictional claims in published maps and institutional affiliations.



Open Access This article is licensed under a Creative Commons Attribution-NonCommercial-NoDerivatives 4.0 International License, which permits any non-commercial use, sharing, distribution and reproduction in any medium or format, as long as you give appropriate credit to the original author(s) and the source, provide a link to the Creative Commons licence, and indicate if you modified the licensed material. You do not have permission under this licence to share adapted material derived from this article or parts of it. The images or other third party material in this article are included in the article's Creative Commons licence, unless indicated otherwise in a credit line to the material. If material is not included in the article's Creative Commons licence and your intended use is not permitted by statutory regulation or exceeds the permitted use, you will need to obtain permission directly from the copyright holder. To view a copy of this licence, visit <http://creativecommons.org/licenses/by-nc-nd/4.0/>.

© The Author(s) 2025